JOURNAL OF GUIDANCE, CONTROL, AND DYNAMICS
Vol. 29, No. 4, July–August 2006

Stability Analysis of a Dynamically Tuned Gyroscope

Jeffrey S. Cain* and Douglas A. Staley†
Carleton University, Ottawa, Ontario K1S 5B6, Canada
and
Glenn R. Heppler‡ and John McPhee‡
University of Waterloo, Waterloo, Ontario N2L 3G1, Canada

Using energy and state space methods, the characteristic equation for a dynamically tuned gyroscope (DTG) is determined and subsequently used in a stability analysis of the system. The stability analysis assumes an ideal system and operation of the DTG within small angles of the nominal position. Finally, stable and unstable configurations of the DTG are demonstrated. The analysis shows that for practical configurations of a DTG, the device is inherently stable.

Nomenclature

I_{gs} = gimbal spin inertia
I_{gt} = gimbal transverse inertia
I_{rs} = rotor spin inertia
I_{rt} = rotor transverse inertia
K_x = stiffness about the gimbal X-axis
K_y = stiffness about the gimbal Y-axis
η = square of the shaft spin rate
θ = Y-axis angular rotation of the rotor with respect to the gimbal
ϕ = X-axis angular rotation of the gimbal with respect to the shaft
Ω = square of the DTG natural frequencies
ω_g = angular velocity of the gimbal
ω_r = angular velocity of the rotor
ω_s = shaft spin rate

I. Introduction

DYNAMICALLY tuned gyroscopes (DTGs) have been in widespread use as instruments for measuring angular position and rates for many years. Recently, the principles of the design have been extended to include momentum management and determination devices used in small satellites.[1] The most common configuration of this device includes a rotor connected to a shaft through a gimbal ring and two sets of orthogonal torsion springs; refer to Fig. 1. Ideally, the rotor would be free from external torques; however, the motion of the gimbal imparts torques on the rotor that can cause high nutation and precession rates. Analyses of the system dynamics[2–4] have shown that through application of the "tuning condition" and maximizing the "Figure of Merit" the effects of the gimbal motion can be minimized but not eliminated.[5–7] These methods force a relationship between the system inertias and spring rates. Further analyses have examined the response of DTGs to angular and linear acceleration inputs.[8,9] Of more significance to this paper, the effect of damping on the stability of DTGs has been examined, with the finding that drag acting on the rotor can cause an instability.[10] The response to this is to have the interior of the DTG at a reduced pressure, limiting the development of air currents.

In general, previous studies have been performed utilizing nonspinning coordinate systems that have been linearized early in the derivation. The result was the identification of three periodic oscillations of the rotor orientation.[6] By delaying linearization of the equations of motion and maintaining a spinning coordinate reference frame until the last step, an additional long-term precession term was extracted.[7]

The referenced papers review the effects of the mechanical properties (i.e., the inertial properties and torsional spring stiffnesses) on the nutation and precession rates of the rotor, but the effect of these properties on the actual stability of the system has not been addressed. This paper addresses the question by deriving the stability boundaries for a DTG using energy methods and a frequency analysis. To retain all of the system's natural frequencies, the derivation is performed in spinning coordinates and linearization occurs after the equations of motion have been derived.

Within this paper it is assumed that the gyro case is fixed in inertial space, and that the rotor and gimbal are symmetric with transverse and spin inertias I_{rt}, I_{rs} and I_{gt}, I_{gs}, respectively. Refer to Fig. 1. The stiffness of the gimbal/shaft and gimbal/rotor connections are represented by K_x and K_y, respectively. It is assumed that the shaft spins at a constant rate, ω_s, and that the mass centres of the components are coincident and fixed. For this idealized model, joint and structural damping are ignored.

II. Equations of Motion for an Idealized Dynamically Tuned Gynoscope

To derive the equations of motion, it is necessary to define the generalized coordinates to be used.[7,11] For the DTG, these coordinates are ϕ, the angle of rotation, about its x-axis, of the gimbal with respect to the shaft, and θ, the angle of rotation of the rotor about its y-axis with respect to the gimbal. Based on these coordinates, the angular velocity of the gimbal can be calculated by rotating the shaft speed, ω_s, into the gimbal coordinate frame and adding the rate about the x-axis. In other words,

$$\omega_g = \begin{pmatrix} \dot{\phi} \\ 0 \\ 0 \end{pmatrix} + (\phi)_x \begin{pmatrix} 0 \\ 0 \\ \omega_s \end{pmatrix}$$

where $(\phi)_x$ represents the rotation matrix of ϕ about the gimbal x-axis. Expanding, the angular rates of the gimbal are found:

$$\omega_{g_x} = \dot{\phi} \tag{1}$$

$$\omega_{g_y} = S_\phi \omega_s \approx \phi \omega_s \tag{2}$$

$$\omega_{g_z} = C_\phi \omega_s \approx \omega_s \tag{3}$$

Received 29 April 2005; revision received 15 November 2005; accepted for publication 15 November 2005.

*Department of Mechanical and Aerospace Engineering; currently Senior Member, Technical Staff, COM DEV, Ltd., Cambridge, Ontario, Canada, N1R 7H6; jeff.cain@ComDev.ca.
†Professor, Department of Mechanical and Aerospace Engineering.
‡Professor, Department of Systems Design Engineering. Senior Member AIAA.

where $S_\phi = \sin\phi$ and $C_\phi = \cos\phi$. The approximations are made by linearizing C_ϕ and S_ϕ about the nominal position $\phi = 0$. Rotating the gimbal angular velocities into the rotor coordinate frame and then adding the rate about the y-axis gives the angular velocity components of the rotor. That is,

$$\omega_r = \begin{pmatrix} 0 \\ \dot{\theta} \\ 0 \end{pmatrix} + (\theta)_y \begin{pmatrix} \omega_{g_x} \\ \omega_{g_y} \\ \omega_{g_z} \end{pmatrix}$$

which expands to give

$$\omega_{r_x} = C_\theta \dot{\phi} - S_\theta C_\phi \omega_s \approx \dot{\phi} - \theta\omega_s \tag{4}$$

$$\omega_{r_y} = \dot{\theta} + S_\phi \omega_s \approx \dot{\theta} + \phi\omega_s \tag{5}$$

$$\omega_{r_z} = S_\theta \dot{\phi} + C_\theta C_\phi \omega_s \approx \omega_s \tag{6}$$

Again, the approximations are valid when θ is small. It is also assumed that the angular rates at these small angles are small compared to ω_s. Now that the angular rates of each of the bodies are known, the kinetic energy $\mathcal{T}$ of the system can be expressed as

$$\mathcal{T} = \tfrac{1}{2}\left[I_{\text{rs}}\omega_{r_z}^2 + I_{\text{rt}}\left(\omega_{r_x}^2 + \omega_{r_y}^2\right) + I_{\text{gs}}\omega_{g_z}^2 + I_{\text{gt}}\left(\omega_{g_x}^2 + \omega_{g_y}^2\right)\right] \tag{7}$$

Also, the potential energy $\mathcal{V}$ is

$$\mathcal{V} = \tfrac{1}{2}K_x\phi^2 + \tfrac{1}{2}K_y\theta^2 \tag{8}$$

Forming the Lagrangian[12] $L = \mathcal{T} - \mathcal{V}$ and applying Lagrange's equations over ϕ and θ yields Eqs. (9) and (10):

$$\frac{\mathrm{d}}{\mathrm{d}t}\left[S_\theta I_{\text{rs}}\omega_{r_z} + C_\theta I_{\text{rt}}\omega_{r_x} + I_{\text{gt}}\omega_{g_x}\right] - (I_{\text{gt}} - I_{\text{gs}})\omega_{g_y}\omega_{g_z}$$
$$- S_\theta I_{\text{rt}}\omega_{g_y}\omega_{r_x} - I_{\text{rt}}\omega_{g_z}\omega_{r_y} + C_\theta I_{\text{rs}}\omega_{g_y}\omega_{r_z} + K_x\phi = 0 \tag{9}$$

$$\frac{\mathrm{d}}{\mathrm{d}t}\left[I_{\text{rt}}\omega_{r_y}\right] - (I_{\text{rs}} - I_{\text{rt}})\omega_{r_x}\omega_{r_z} + K_y\theta = 0 \tag{10}$$

Equation (9) can be simplified by realizing $\omega_{g_x} = C_\theta\omega_{r_x} + S_\theta\omega_{r_z}$, giving

$$C_\theta(I_{\text{rt}} + I_{\text{gt}})\dot{\omega}_{r_x} + S_\theta(I_{\text{rs}} + I_{\text{gt}})\dot{\omega}_{r_z} - \dot{\theta}\left(S_\theta I_{\text{rt}}\omega_{r_x} - C_\theta I_{\text{rs}}\omega_{r_z}\right.$$
$$\left. + \left(S_\theta\omega_{r_x} - C_\theta\omega_{r_z}\right)I_{\text{gt}}\right) - (I_{\text{gt}} - I_{\text{gs}})\omega_{g_y}\omega_{g_z}$$
$$- \left(S_\theta I_{\text{rt}}\omega_{r_x} - C_\theta I_{\text{rs}}\omega_{r_z}\right)\omega_{g_y} - I_{\text{rt}}\omega_{g_z}\omega_{r_y} + K_x\phi = 0 \tag{11}$$

Using the relationships $S_\theta\omega_{r_x} - C_\theta\omega_{r_z} = -\omega_{g_z}$ and $\dot{\theta} + \omega_{g_y} = \omega_{r_y}$ in Eq. (11) and expanding Eq. (10) gives the equations of motion as

$$C_\theta(I_{\text{rt}} + I_{\text{gt}})\dot{\omega}_{r_x} + S_\theta(I_{\text{rs}} + I_{\text{gt}})\dot{\omega}_{r_z} + \left(C_\theta I_{\text{rs}}\omega_{r_z} - S_\theta I_{\text{rt}}\omega_{r_x}\right.$$
$$\left. + I_{\text{gt}}\omega_{g_z}\right)\omega_{r_y} - (2I_{\text{gt}} - I_{\text{gs}})\omega_{g_y}\omega_{g_z} - I_{\text{rt}}\omega_{g_z}\omega_{r_y} + K_x\phi = 0 \tag{12}$$

and

$$I_{\text{rt}}\dot{\omega}_{r_y} - (I_{\text{rs}} - I_{\text{rt}})\omega_{r_x}\omega_{r_z} + K_y\theta = 0 \tag{13}$$

Using the small-angle assumption and replacing the rotor and gimbal angular rates with Eqs. (1) through (6) gives

$$(I_{\text{rt}} + I_{\text{gt}})\ddot{\phi} + (I_{\text{rs}} - 2I_{\text{rt}})\omega_s\dot{\theta} + \left((I_{\text{gs}} - I_{\text{gt}} + I_{\text{rs}} - I_{\text{rt}})\omega_s^2 + K_x\right)\phi = 0 \tag{14}$$

and

$$I_{\text{rt}}\ddot{\theta} - (I_{\text{rs}} - 2I_{\text{rt}})\omega_s\dot{\phi} + \left((I_{\text{rs}} - I_{\text{rt}})\omega_s^2 + K_y\right)\theta = 0 \tag{15}$$

These equations can be rewritten in matrix form as

$$\boldsymbol{M}\begin{bmatrix}\ddot{\phi}\\ \ddot{\theta}\end{bmatrix} + \boldsymbol{G}\begin{bmatrix}\dot{\phi}\\ \dot{\theta}\end{bmatrix} + \boldsymbol{K}\begin{bmatrix}\phi\\ \theta\end{bmatrix} = \begin{bmatrix}0\\ 0\end{bmatrix} \tag{16}$$

where

$$\boldsymbol{M} = \begin{bmatrix} I_{\text{rt}} + I_{\text{gt}} & 0 \\ 0 & I_{\text{rt}} \end{bmatrix} \tag{17}$$

$$\boldsymbol{G} = \begin{bmatrix} 0 & (\delta I_r - I_{\text{rt}})\omega_s \\ -(\delta I_r - I_{\text{rt}})\omega_s & 0 \end{bmatrix} \tag{18}$$

$$\boldsymbol{K} = \begin{bmatrix} K_x + (\delta I_g + \delta I_r)\omega_s^2 & 0 \\ 0 & K_y + \delta I_r\omega_s^2 \end{bmatrix} \tag{19}$$

and with $\delta I_r = (I_{\text{rs}} - I_{\text{rt}})$ and $\delta I_g = (I_{\text{gs}} - I_{\text{gt}})$.

At this point, it should be noted that the state space form has been used to allow the use of standard stability analysis techniques. In addition, the equations have been kept in a spinning coordinate frame to prevent the loss of significant terms. The necessity of this is demonstrated by placing the equations of motion in the nonspinning coordinate frame. The complete derivation will not be shown in this paper; however, the complex variable technique is used[2,7] to put the equations in a more meaningful form. Once Eqs. (12) and (13) are combined, transformation from nonspinning, or case-fixed, to spinning coordinates is achieved through the multiplication by[2,7] $e^{-j\omega_s t}$, where $j = \sqrt{-1}$. The relationships between the nonspinning and the spinning coordinates are then

$$q = q_x + jq_y$$
$$= e^{j\omega_s t}(\phi + j\theta)$$

with its complex conjugate as

$$\bar{q} = e^{-j\omega_s t}(\phi - j\theta)$$

Note that the complex angle q is made up of small Euler angles, whereas the sensors, or pickoffs, that measure the rotor orientation in a DTG actually measure a distance from a case reference to the rotor rim. In the case of the DTG, the difference between these angles is usually so small that the errors may be ignored.

In the nonspinning coordinate frame, the equations of motion can be reduced to

$$\ddot{q} - j\omega_n\dot{q} + \alpha_{ns}q + [\gamma_{ns}(\ddot{q} + 2j\omega_s\dot{q}) + \beta_{ns}q]e^{2j\omega_s t} = 0 \tag{20}$$

where

$$\omega_n = \frac{I_{\text{rs}} + I_{\text{gt}}}{I_{\text{rt}} + I_{\text{gt}}/2}\omega_s$$

$$\alpha_{ns} = \frac{K_x + K_y - (2I_{\text{gt}} - I_{\text{gs}})\omega_s^2}{2I_{\text{rt}} + I_{\text{gt}}}$$

$$\gamma_{ns} = \frac{I_{\text{gt}}}{2I_{\text{rt}} + I_{\text{gt}}}$$

$$\beta_{ns} = \frac{K_x - K_y - (2I_{\text{gt}} - I_{\text{gs}})\omega_s^2}{2I_{\text{rt}} + I_{\text{gt}}}$$

Together with its complex conjugate, Eq. (20) can be used to determine the equations for both q and $\bar{q}$. However, inspection of this single equation can be informative. The terms within the brackets are modulated at twice the spin speed and include coefficients that depend on the ratio between the gimbal and rotor inertias. Because the gimbal is very small compared to the rotor, these terms are typically ignored, resulting in the equation

$$\ddot{q} - j\omega_n\dot{q} + \alpha_{ns}q \approx 0$$

which reflects a free rotor if $\alpha_{ns} = 0$. This is obtained by setting

$$K_x + K_y - (2I_{\text{gt}} - I_{\text{gs}})\omega_s^2 = 0$$

which is the tuning condition mentioned previously. However, when the terms in γ_{ns} and β_{ns} are not ignored, a very low-frequency response is found.[7] This implies that low-frequency precession would be expected, because a pure null would not be possible in practice. With a rebalance control loop around the gyro, and with a null that does not perfectly match the mechanical null, the low-frequency precision shows up as a drift rate. This drift has, in the past, raised debates over the stability of DTGs.

By maintaining the equations of motion within the rotating coordinate frame, the rotating terms are kept and the stability of the system can be evaluated. In general, the solution of Eq. (16) has the form

$$\begin{bmatrix}\phi\\ \theta\end{bmatrix} = \boldsymbol{A}e^{j\omega t} \tag{21}$$

and can be rewritten as

$$\{-\omega^2\boldsymbol{M} + j\omega\boldsymbol{G} + \boldsymbol{K}\}\boldsymbol{A}e^{j\omega t} = \begin{bmatrix}0\\ 0\end{bmatrix} \tag{22}$$

The characteristic equation of the system can be written as

$$\Delta = \det(-\omega^2\boldsymbol{M} + j\omega\boldsymbol{G} + \boldsymbol{K}) \tag{23}$$

$$= I_{\mathrm{rt}}(I_{\mathrm{rt}} + I_{\mathrm{gt}})\Omega^2 - \Big((I_{\mathrm{rt}}(K_x + K_y) + I_{\mathrm{gt}}K_y) + \Big(I_{\mathrm{rt}}\delta I_g - 2\delta I_r I_{\mathrm{rs}}^2 + I_{\mathrm{gt}}\delta I_r\Big)\eta\Big)\Omega + (K_x + (\delta I_g + \delta I_r)\eta)(K_y + \delta I_r\eta) = 0 \tag{24}$$

where $\Omega = \omega^2$ and $\eta = \omega_s^2$. Of note is that ω_s only appears in the quadratic form (ω_s^2), indicating that the direction of rotation has no effect on the stability behavior of the DTG. The quantity η will be referred to as the shaft speed and, because there is little possibility of confusion, Ω will be referred to as the frequency. The characteristic equation is now in a form that can be used for a stability analysis.

III. Stability Analysis

Since the solution of the equations of motion are assumed to have the form $\boldsymbol{A}e^{j\omega t}$, it is necessary that Ω, the square of the roots of the characteristic equation (24), be positive and real for the system to be stable.

Given that ω represents the natural or fundamental frequencies of the system, if $\Omega \in \Re$ and $\Omega < 0$ then the roots ω are imaginary conjugates and one value of $j\omega$ will be positive real. This results in an exponentially growing mode and a corresponding instability due to divergence. If Ω is positive and real, it is still possible for the system to be unstable. This occurs when the roots ω are complex conjugates where the real parts will contribute to oscillatory behavior in the modes and the imaginary parts will result in one of the modes decaying to zero and the other growing exponentially. The growing oscillatory mode is a flutter instability.[13] For a DTG, a divergent mode would be represented by an exponential increase in the gimbal angles. Flutter instability would manifest itself as growing, oscillatory gimbal angles.

Normalizing with respect to the rotor transverse inertia, Eq. (24) can be rewritten as

$$\Delta(\Omega) = \alpha\Omega^2 - (\beta + \Upsilon\eta)\Omega + (K_x/I_{\mathrm{rt}} + \Psi\eta)(K_y/I_{\mathrm{rt}} + \Gamma\eta) = 0 \tag{25}$$

where

$$\alpha = 1 + I_{\mathrm{gt}}/I_{\mathrm{rt}} \tag{26}$$

$$\beta = (K_x + K_y)/I_{\mathrm{rt}} + I_{\mathrm{gt}}K_y\Big/I_{\mathrm{rt}}^2 \tag{27}$$

$$\Upsilon = 1 + (I_{\mathrm{gs}} - 2I_{\mathrm{gt}})/I_{\mathrm{rt}} + I_{\mathrm{gt}}I_{\mathrm{rs}}\Big/I_{\mathrm{rt}}^2 + (I_{\mathrm{rs}}/I_{\mathrm{rt}} - 1)^2 \tag{28}$$

$$\Psi = (I_{\mathrm{gs}} + I_{\mathrm{rs}} - I_{\mathrm{gt}})/I_{\mathrm{rt}} - 1 = (\delta I_g + \delta I_r)/I_{\mathrm{rt}} \tag{29}$$

$$\Gamma = I_{\mathrm{rs}}/I_{\mathrm{rt}} - 1 = \delta I_r/I_{\mathrm{rt}} \tag{30}$$

As stated earlier, the system will experience a divergent instability if one, or both, of the roots of the characteristic equation (25) are less than zero (Ω_1 or $\Omega_2 < 0$). The boundary between the stable regions and the divergence unstable regions, known as the divergence boundary, is found from the condition[13,14]

$$\Delta(\Omega) = 0 \qquad \text{when} \qquad \Omega_i = 0 \qquad i = 1 \text{ or } 2 \tag{31}$$

For at least one root of the characteristic equation to be zero, it is necessary that

$$(K_x/I_{\mathrm{rt}} + \Psi\eta)(K_y/I_{\mathrm{rt}} + \Gamma\eta) = 0$$

or

$$(K_x + (\delta I_g + \delta I_r)\eta)(K_y + \delta I_r\eta) = 0 \tag{32}$$

This equation for the divergence boundary can be expanded into a second-order polynomial involving the shaft speed η, which has the two roots

$$\eta_1 = -K_y/\delta I_r \tag{33}$$

$$\eta_2 = -K_x/(\delta I_g + \delta I_r) \tag{34}$$

Values of $\eta_i < 0$ are not physically realizable, so only those circumstances that lead to $\eta_i \geq 0$ in Eqs. (33) or (34) are of interest. This can occur only if

$$\delta I_r = (I_{\mathrm{rs}} - I_{\mathrm{rt}}) < 0$$

or

$$\delta I_g + \delta I_r = (I_{\mathrm{gs}} - I_{\mathrm{gt}} + I_{\mathrm{rs}} - I_{\mathrm{rt}}) < 0$$

neither of which is likely to occur for physically realistic systems, where the design standard is to have the spin inertia greater than the transverse inertia.

Alternatively, the divergence boundary condition (32) may be viewed as a quadratic in terms of δI_r, which has the roots

$$\delta I_{r1} = -K_y/\eta \tag{35}$$

$$\delta I_{r2} = -(\eta\delta I_g + K_x)/\eta \tag{36}$$

Again it is possible, but unlikely in practice, for $\delta I_{r1} < 0$ or $\delta I_{r2} < 0$, so these divergence boundaries are feasible but are unlikely to be encountered.

Finally, the divergence boundary condition (32) may be viewed as linear in δI_g, which yields the single root

$$\delta I_g = -(\delta I_r\eta + K_x)/\eta \tag{37}$$

which is also feasible but unlikely in practice. It should be noted that if both of the roots of the characteristic equation (25) are to be zero then it would be necessary for

$$\beta + \Upsilon\eta = 0 \tag{38}$$

or

$$\Big(\delta I_r^2 + I_{\mathrm{gt}}\delta I_r + I_{\mathrm{rt}}^2 + \delta I_g I_{\mathrm{rt}}\Big)\eta + K_x I_{\mathrm{rt}} - (I_{\mathrm{rt}} + I_{\mathrm{gt}})K_y = 0 \tag{39}$$

which can never occur for a practical gyroscope where the spin inertia is greater than the transverse inertia and the stiffness of the torsional springs is equal and positive.

If the roots of the characteristic equation are complex then the system will lose stability because of flutter.[13] The flutter boundaries can be determined by satisfying the equations

$$\Delta(\Omega) = 0 \tag{40}$$

$$\frac{\partial\Delta(\Omega)}{\partial\Omega} = 0 \tag{41}$$

Using the characteristic equation (25)

$$\frac{\partial\Delta}{\partial\Omega} = 2\alpha\Omega - (\beta + \Upsilon\eta) \tag{42}$$

The roots of the characteristic equation are

$$\Omega_{1,2} = (1/2\alpha)\Big[(\beta + \Upsilon\eta) \pm \Big((\beta + \Upsilon\eta)^2 - 4\alpha(K_x/I_{\mathrm{rt}} + \Psi\eta)(K_y/I_{\mathrm{rt}} + \Gamma\eta)\Big)^{\frac{1}{2}}\Big] \tag{43}$$

The roots from Eq. (43) can now be substituted into Eq. (42), which is then squared, and the resulting equation for the flutter boundary is

$$(\beta + \Upsilon\eta)^2 - 4\alpha(K_x/I_{\mathrm{rt}} + \Psi\eta)(K_y/I_{\mathrm{rt}} + \Gamma\eta) = 0 \tag{44}$$

Equation (44) can be expanded to give

$$(\Upsilon^2 - 4\alpha\Gamma\Psi)\eta^2 + \{2\beta\Upsilon - 4\alpha[(K_x\Gamma + K_y\Psi)/I_{\mathrm{rt}}]\}\eta + \Big[\beta^2 - 4\alpha\Big(K_xK_y\Big/I_{\mathrm{rt}}^2\Big)\Big] = 0 \tag{45}$$

Again, this situation would not be encountered in a practical gyroscope because the relationship is only true for negative values of η, which are not physically realizable. Therefore, flutter instability would not be encountered in service.

A special case worth examining occurs when the pivots are replaced with bearings. This scenario represents early models of the DTG. In this case, the stiffness of the pivots is zero. With $K_x = K_y = 0$, the characteristic equation becomes

$$\alpha\Omega^2 - \Upsilon\eta\Omega + \Gamma\Psi\eta^2 = 0 \tag{46}$$

The roots of Eq. (46) are

$$\Omega = (\eta/2\alpha)\Big(\Upsilon \pm \sqrt{\Upsilon^2 - 4\alpha\Gamma\Psi}\Big)$$

For the system to be unstable by divergence, it is necessary that one of the roots of the characteristic equation be less than zero. By definition, $\alpha > 1$, which means that for this to occur

$$\sqrt{\Upsilon^2 - 4\alpha\Gamma\Psi} > \Upsilon$$

This can be rewritten in the form

$$\alpha\Gamma\Psi < 0$$

Given the restriction on α stated earlier, this equation is only true if either Γ or Ψ is negative, but not both. Therefore, using the definitions of Ψ and Γ in Eqs. (29) and (30), the region of instability of the DTG is

$$I_{\mathrm{rs}} < I_{\mathrm{rt}} < I_{\mathrm{rs}} + I_{\mathrm{gs}} - I_{\mathrm{gt}}$$

which is a very limited and unusual distribution of inertias. Thus, it has been shown there is only a small region where a DTG with bearings would be unstable by divergence. There is also the possibility that the DTG could become unstable through flutter. This can be checked by determining if the roots of characteristic equation (46) are complex. This will only be true if

$$\Upsilon^2 - 4\alpha\Gamma\Psi < 0$$

or

$$\Upsilon^2 < 4\alpha\Gamma\Psi$$

This condition is not likely to be encountered in a DTG. It is clear that it is unlikely for a DTG to become unstable, even when operating in a untuned condition such as that found when "pins and jewels" or bearings are used in the place of flexure pivots.

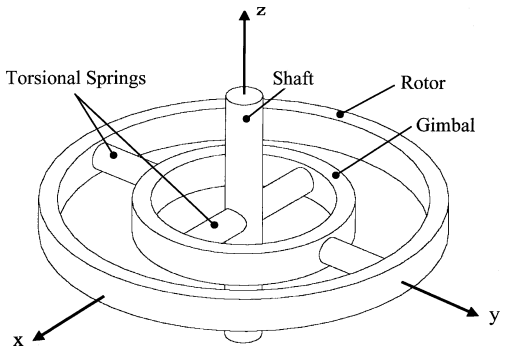

Fig. 1 Schematic of a dynamically tuned gyro showing the rotor and gimbal rings, shaft, and torsional elements.

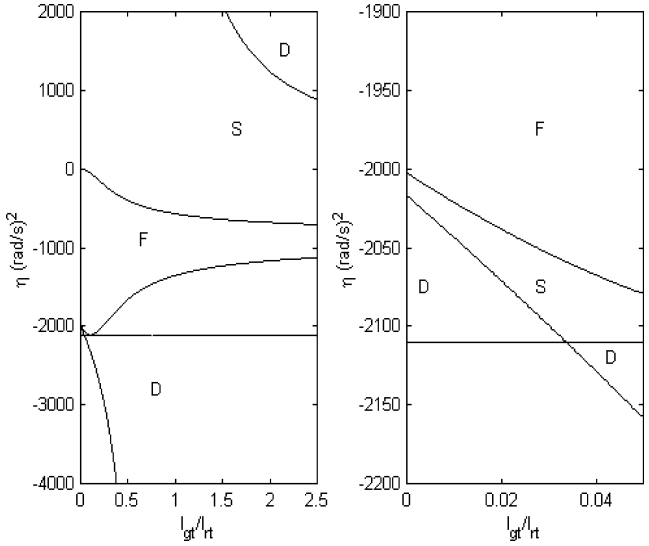

Fig. 2 Stability boundaries for a gyro with varying gimbal transverse inertia. D represents divergence, S represents a stable region, and F represents an unstable system due to flutter.

IV. Numerical Study

At this point it is possible to perform a numerical study to observe the effect of changing various parameters on the stability of a typical DTG with flexure pivots, the properties of which are given in Table 1. The study is performed by changing the value of one parameter while keeping the remaining ones constant. Although negative values of η are plotted, these values are physically impossible to achieve and are only shown to give a clear understanding of the trends of the curves.

For presentation purposes, only one case will be evaluated. The remaining cases can be found by using a similar method and varying other parameters. This study involves changing the value of the gimbal transverse inertia, I_{gt}. Figure 2 gives the stability boundaries of the system. For feasible values of η, it is only possible for the system to go unstable by divergence when the ratio of the gimbal to rotor transverse inertia is greater than one and at shaft spin speeds greater than 30 rad/s. From Fig. 2 it is observed that the value of η at which flutter occurs decreases as the transverse inertia of the gimbal increases from the tuned value. The flutter boundary remains fairly constant for values of transverse inertia smaller than that shown in Table 1.

For the chosen example, the tuning condition[2] gives $\eta = 440{,}000$ $(\mathrm{rad/s})^2$. This places the operating condition for the gyro in the upper left hand quadrant of the plot (off the scale) and well away from the divergent boundary. Note that the divergent boundary approaches a ratio of gimbal to rotor transverse inertia of one for high values of η. From this analysis, it can be seen that the system will remain stable for all reasonable operating conditions.

It should be noted in this case that the system does not enter a region of flutter instability. Additional studies have shown that the

Table 1 Inertial and stiffness properties of a typical dynamically tuned gyro

Parameter	Value	Units
I_{rs}	70.0	g cm^2
I_{rt}	40.5	g cm^2
I_{gs}	1.37	g cm^2
I_{gt}	0.8267	g cm^2
K_x	6.226×10^4	dyn cm/rad
K_y	6.226×10^4	dyn cm/rad

gyro only enters regions of divergent instability in extreme cases where, for example, the stiffness of the torsional springs have a very large negative value or the transverse inertia of the gimbal is quite large. In fact, it can be shown that, for a practical gyro design, the system would be stable. The stability of the gyro is insensitive to practical changes in the physical properties of the system.

V. Conclusions

Well documented in the literature, application of the tuning equation to the design of the dynamically tuned gyroscope (DTG) removes the first-order effects of the gimbal motion. However, second-order effects still remain and influence the response of the rotor. This response is not an unstable condition and reflects a stable precession and nutation of the rotor. However, in the past, this response has led to the belief that the rotor was unstable.

This paper contains a stability analysis of a dynamically tuned gyroscope. With these equations, it can be shown that, for all practical configurations, the DTG is inherently stable when operated at low angular offsets. In fact, it was found that large deviations from the tuning condition were required for system instability.

References

[1]Tyc, G., Staley, D. A., Cain, J. S., Ower, J. C., Wiktowy, M., Pradham, S., and Whitehead, W. R., "The Momentum Management System (MMS)—An Innovative New Device for 3-Axis Spacecraft Attitude Control," Canadian Aeronautics and Space Institute Conference, Canadian Aeronautics and Space Institute, Ottawa, Oct. 1998.

[2]Craig, R. J. G., "Theory of Operation of an Elastically Supported, Tuned Gyroscope," *IEEE Transactions on Aerospace and Electronic Systems*, Vol. AES-8, No. 3, 1972, pp. 280–288.

[3]Lawrence, A. W., "A Simulation of a Dynamically Tuned Gyroscope," *Gyrodynamics: Euromech 38 Colloquim*, edited by P. Y. Willems, Springer-Verlag, New York, 1974, pp. 56–62.

[4]Burdess, J. S., and Fox, C. H. J., "The Dynamics of a Multigimbal Hooke's-Joint Gyroscope," *The Journal of Mechanical Engineering Science*, Vol. 20, No. 5, 1978, pp. 255–262.

[5]Fogarasy, A. A., "A Contribution to the Dynamics of a Spring Restrained Hooke's Joint Gyroscope," *Gyrodynamics: Euromech 38 Colloquim*, Springer-Verlag, New York, 1974, pp. 49–55.

[6]Lawrence, A., *Modern Inertial Technology*, 2nd ed., Springer-Verlag, New York, 1993, pp. 127–147.

[7]Staley, D., and Cain, J. S., "Dynamics of a Tuned Rotor Gyroscope," *Canadian Aeronautics and Space Journal*, Vol. 43, No. 2, 1997, pp. 106–110.

[8]Craig, R. J. G., "Theory of Errors of a Multigimbal, Elastically Tuned Gyroscope," *IEEE Transactions on Aerospace and Electronic Systems*, Vol. AES-8, No. 3, 1972, pp. 289–297.

[9]Burdess, J. S., Fox, C. H. J., and Maunder, L., "The Response of a Hooke's-Joint Gyroscope to Linear Vibration," *The Journal of Mechanical Engineering Science*, Vol. 20, No. 4, 1978, pp. 189–195.

[10]Burdess, J. S., and Fox, C. H. J., "The Dynamics of an Imperfect, Multigimbal, Hooke's-Joint Gyroscope," *The Journal of Mechanical Engineering Science*, Vol. 20, No. 5, 1978, pp. 263–269.

[11]Cain, J. S., "Investigation of the Crossed Flexure Pivot and the Dynamics of the Momentum Management System Spacecraft Control Component and the Dynamically Tuned Gyroscope," Ph.D Dissertation, Department of Mechanical and Aerospace Engineering, Carleton University, Ottawa, Canada, 1999.

[12]Hildebrand, F. B., *Methods of Applied Mathematics*, 2nd ed., Prentice–Hall, Engelwood Cliffs, NJ, 1992, pp. 151–165.

[13]Yamanaka, K., "On the Stability Analysis of Gyroelastic Systems," Ph.D Dissertation, Univ. of Waterloo, Waterloo, Canada, 1993.

[14]Huseyin, K. *Vibrations and Stability of Multiple Parameter Systems*, Noordhoff International Publishing, The Netherlands, 1978, Chaps. 2, 3, and 5.